Rare Met. (2018) 37(5):376–380
https://doi.org/10.1007/s12598-016-0768-6

RARE METALS
www.editorialmanager.com/rmet

Transformation and dissolution of second phases during solution treatment of an Al–Zn–Mg–Cu alloy containing high zinc

Kai Wen, Bai-Qing Xiong*, Yun-Qiang Fan, Yong-An Zhang, Zhi-Hui Li, Xi-Wu Li, Feng Wang, Hong-Wei Liu

Received: 11 June 2015 / Revised: 2 August 2015 / Accepted: 17 May 2016 / Published online: 21 June 2016

Abstract The transformation and dissolution of Mg(Zn, Cu, Al)$_2$ phase during solution treatment of an Al–Zn–Mg–Cu alloy containing high zinc were investigated by means of optical microscopy (OM), scanning electron microscopy (SEM), energy-dispersive X-ray spectrometry (EDX) and X-ray diffraction (XRD). The results show that solution temperature is the main factor influencing phase dissolution. With solution temperature increasing, the content of residual phases decreases. Phase transformation from Mg(Zn, Cu, Al)$_2$ to S(Al$_2$CuMg) occurs under solution temperature of 450, 460 and 465 °C. Mg(Zn, Cu, Al)$_2$ phase is directly dissolved into the matrix under solution temperature of 470 and 475 °C, and no S(Al$_2$CuMg) phase transformed from Mg(Zn, Cu, Al)$_2$ phase is observed. The formation of S(Al$_2$CuMg) phase is mainly controlled by Zn elemental diffusion. The mechanism of transformation and dissolution of second phases was investigated. At low temperature, the dissolution of Zn is faster than that of Mg and Cu, resulting in an appropriate condition to form S(Al$_2$CuMg) phase. At high temperature, the dissolution of main alloying elements has no significant barrier among them to form S(Al$_2$CuMg) phase.

Keywords Al–Zn–Mg–Cu alloy; Microstructure; Solution treatment; Phase transformation

K. Wen, B.-Q. Xiong*, Y.-Q. Fan, Y.-A. Zhang, Z.-H. Li, X.-W. Li, F. Wang, H.-W. Liu
State Key Laboratory of Nonferrous Metals and Processes, General Research Institute for Nonferrous Metals, Beijing 100088, China
e-mail: xiongbq@grinm.com

1 Introduction

Al–Zn–Mg–Cu alloy plates are widely used in the aeronautical and aerospace industries in consideration of a good combination of specific strength, hot workability, toughness and fatigue durability [1, 2]. Although the properties of Al–Zn–Mg–Cu alloys are very attractive, the processing of these alloys is quite difficult due to their high alloying element contents. The properties of these alloy plates can be optimized by applying a series of treatments, including solution, quenching and aging heat-treatments [3, 4]. Generally, the solution treatment is a primary and key step [5–7]. During the solution treatment, soluble phases can be re-dissolved into the matrix to form supersaturated solid solution, preparing for subsequent aging treatment. At a higher solution temperature, soluble phases can re-dissolve more sufficiently. However, for the single-stage solution treatment, the solution temperature should be below the incipient melting point for Mg(Zn, Cu, Al)$_2$ phase. Otherwise, the alloy may be over-burnt, which is detrimental to mechanical performance. Besides, a solution process at high temperatures led to severe recrystallization and a decrease in the strength, toughness and even a resistance to corrosion of the aged materials [8–10]. Hence, to avoid severe recrystallization and get good overall performance after aging treatments, a preferential solution treatment regime should choose relatively low temperature on the basis of ensuring the re-dissolution of soluble phase.

Previous literatures chiefly focused on the adjustment of process temperature and time period to get superior microstructure and simply described phase species in alloys after solution treatment. Mazibuko and Curle [11] found that S(Al$_2$CuMg) phase occurred after solution treatment at 473 °C. Deng et al. [6] also found that the specimen contained Al$_2$CuMg particles for temperature up

to 475 °C. On the other hand, Han et al. [7] asserted that the Mg(Zn, Cu, Al)$_2$ phase directly dissolved into the matrix during solution treatment and no S(Al_2CuMg) phase was found. Apparently, the mechanism of phase dissolution or transition during solution treatment has received little attention. Hence, it is obliged to systemically clarify them.

In this paper, the transformation and dissolution of the second phases during solution treatment under various temperature regimes were studied. The present study was focused on the effect of the gap between Zn and Cu elemental diffusion rate on the Mg(Zn, Cu, Al)$_2$ phase dissolution and its transition during solution treatment. The results could give indispensable information for optimizing the solution processing parameters.

2 Experimental

The present study was carried out on the 25-mm-thick hot extruded Al–Zn–Mg–Cu alloy plate with chemical composition of Al–8.02Zn–1.80Mg–2.02Cu–0.15Zr–0.046Fe (wt%). Solution treatments were conducted in air using a resistance-heated box furnace with forced air convection. The solution treatment procedures are listed in Table 1. The samples for metallographic observation were prepared through a conventional mechanical polishing and followed by etching with Graff Seagent solution (1 ml HF, 16 ml HNO_3, 3 g CrO_3 and 83 ml water). The metallographic observation was performed on optical microscopy (OM, Zeiss Axiovert 200 MAT). The morphology of the residual phase was examined on a scanning electron microscope (SEM, JEOL JSM 7001F). The second-phase particles were identified by energy-dispersive X-ray spectrometry (EDX). To quantitatively evaluate the dissolution of constituent particles, SEM images were taken at least ten random sites for each sample. By using Image-Pro Plus software, the content of remaining constituents in as-extruded and different solution-treated samples was determined. The microstructural characterization was carried out by X-ray diffractometer (XRD, Rigaku D/Max 2500) with 0.5° step. The content of the second-phase particles was measured on the SEM micrographs by using point counting with a grid containing 900 points [12]. The conductivity of the alloy at different conditions was measured by a WD-Z eddy current conductivity meter with at least five random sites for each sample.

Table 1 Solution treatment schedules of as-extruded plate of Al–Zn–Mg–Cu alloy

Samples	Solution treatment schedules
SHT450	450 °C/2 h
SHT460	460 °C/2 h
SHT465	465 °C/2 h
SHT470	470 °C/2 h
SHT475	475 °C/2 h

3 Results and discussion

3.1 Observation of as-extruded microstructure

The microstructures of as-extruded Al–Zn–Mg–Cu alloy plate are shown in Fig. 1. It can be observed that a number of coarse second-phase particles distribute along the extruding direction. The EDS analysis reveals that these second particles are Mg(Zn, Cu, Al)$_2$ phase and Fe-rich phase (Table 2). Large amounts of fine white phase are distributed homogenously in the matrix (Fig. 1b). According to the EDS results, they are also Mg(Zn, Cu, Al)$_2$ phases. The XRD pattern of as-extruded Al–Zn–Mg–Cu alloy (Fig. 2) also proves that the primary phases are α(Al) and the phases with crystal structure of $MgZn_2$. Most second-phase particles are expected to be dissolved into the matrix by the solution treatment. However, the high

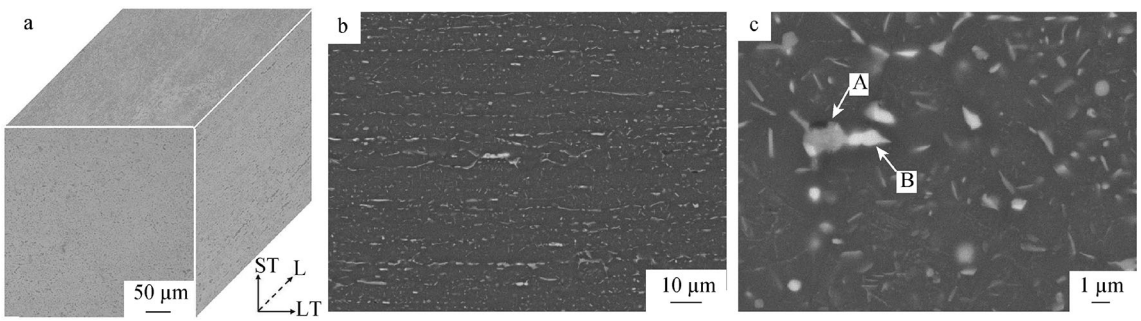

Fig. 1 Morphologies of second-phase particles of as-extruded alloy: **a** OM image, **b** SEM image on longitudinal plane, and **c** high-magnitude SEM image on longitudinal plane with phases labeled by EDS. L, LT and ST being longitudinal direction, long-transverse direction and short-transverse direction, respectively

Table 2 EDX results of second-phase particles of as-extruded plate from Fig. 1 (at%)

Points	Al	Zn	Mg	Cu	Fe
A	72.36	3.51	5.83	8.27	3.54
B	62.70	12.53	13.99	6.57	–

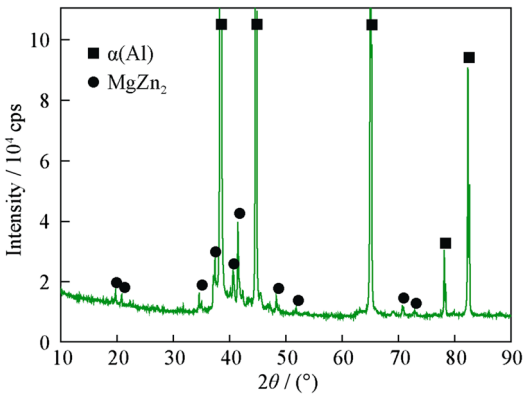

Fig. 2 XRD pattern of as-extruded alloy

temperature of the solution treatment inevitably increases recrystallization proportion. Therefore, it is necessary to optimize the solution treatment.

3.2 Dissolution of constituent particles

The typical micrographs of the alloy after solution treatment at different conditions are shown in Fig. 3. The corresponding EDS analysis is shown in Table 3. The S(Al_2CuMg) phase is observed in Samples SHT450, SHT460 and SHT465 (Points A, C, E, F and G in Fig. 3). According to the contrast of different phases of SEM images, few Mg(Zn, Cu, $Al)_2$ phases still remain in Samples SHT450 and SHT460 (Points B, D in Fig. 3). No (Al_2CuMg) phase is detected in as-extruded sample. Hence, it can be explained that S(Al_2CuMg) phase transforms from Mg(Zn, Cu, $Al)_2$ phase during solution treatments. This is in agreement with literatures on solution treatments [13]. Only Fe-rich phase is observed in the microstructure of Samples SHT470 and SHT475. It is necessary to note that Fe-rich phase is also observed in Samples SHT450, SHT460 and SHT465, which is just not marked in the micrographs. To get a better view, the phase existence of samples solution-treated in different conditions is shown in Table 4. Various phases are labeled as "Y" for the existence and "N" for the inexistence. It can be obviously seen from the micrographs that the SHT samples treated at high temperatures possess less residual phases. In general, compared to the as-extruded alloy plate,

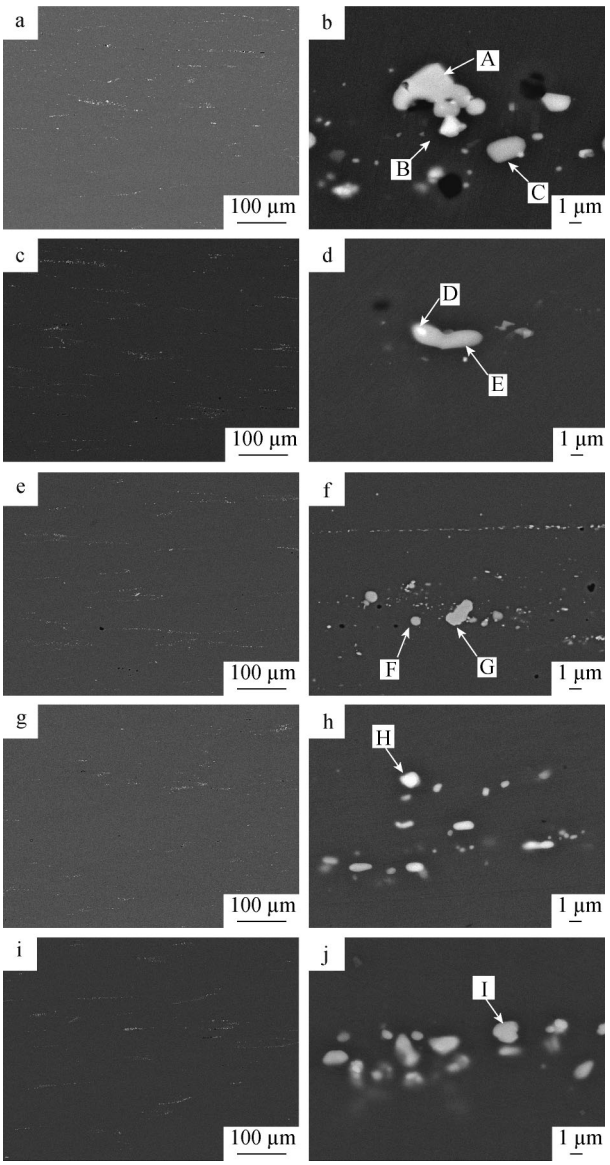

Fig. 3 SEM images of as-extruded alloy after solution-treated at different conditions: **a**, **b** SHT450; **c**, **d** SHT460; **e**, **f** SHT465; **g**, **h** SHT470; and **i**, **j** SHT475

the fine secondary phase particles are dissolved into the matrix of SHT samples.

The conductivity of the alloy at different conditions was also measured, as shown in Fig. 4. Typically, the conductivity is used to indicate the supersaturation level of alloys. Compared to the as-extruded samples, the conductivity of the SHT samples exhibits a significant decrement. Besides, the conductivity decreases with the solution temperature increasing for Samples SHT450, SHT460, SHT465 and SHT470. That means a sustainable increment of the supersaturation of the matrix, namely the second-phase dissolution, occurs all the time. This is in accordance with the SEM observation. For Sample SHT475, the

Table 3 EDX analysis of constituent phases in Fig. 3 (at%)

Points	Al	Zn	Mg	Cu	Fe
A	62.92	2.05	18.65	16.38	–
B	64.53	23.84	2.33	9.30	–
C	82.25	–	9.41	8.34	–
D	69.77	7.14	13.98	9.10	–
E	73.80	2.37	12.24	11.59	–
F	66.95	2.61	15.99	14.46	–
G	51.50	2.40	24.64	21.46	–
H	88.53	–	2.36	6.52	2.59
I	82.13	–	2.15	10.83	4.90

Table 4 Phase existence in as-extruded samples after solution treatment at different temperatures

Samples	$Mg(Zn, Cu, Al)_2$	$S(Al_2CuMg)$	Fe-rich phase
SHT450	Y	Y	Y
SHT460	Y	Y	Y
SHT465	N	Y	Y
SHT470	N	N	Y
SHT475	N	N	Y

Y: existence, N: inexistence

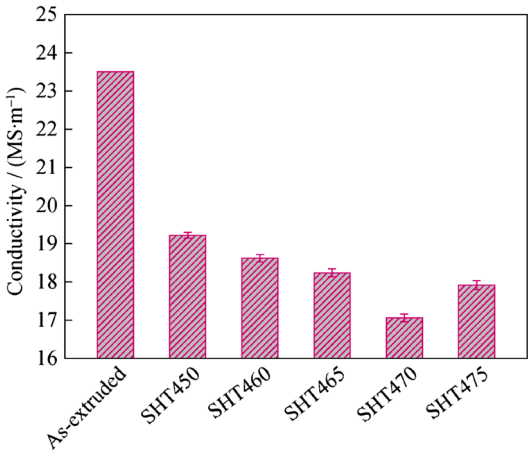

Fig. 4 Conductivity of as-extruded alloy at different conditions

conductivity is higher than that of Sample SHT470. This can be explained that an increment of solution temperature is not beneficial to the supersaturation of the matrix, which means that an enhanced temperature is not necessary for phase dissolution. Corresponding to the SEM observation in Fig. 3, both Samples SHT470 and SHT475 only have Fe-rich phase.

In order to quantitatively analyze phase dissolution, the content of the second-phase particles treated at different conditions was statistically measured, as shown in Fig. 5.

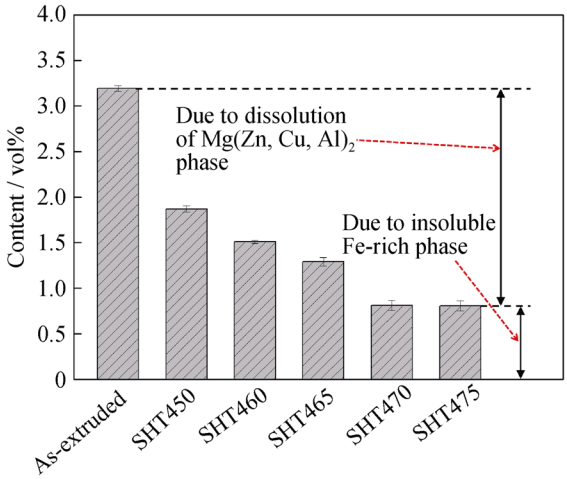

Fig. 5 Content of second-phase particles of as-extruded alloy after solution treatment at different temperatures

The results show that solution treatment has a significant effect on phase dissolution. After holding for 2 h at 450 °C, the content of constituent particles in the alloy drops rapidly from 3.19 vol% to 1.87 vol%. The content of residual phases decreases with the solution temperature increasing for SHT samples. The content of residual phases in Sample SHT470 is 0.81 vol%, basically stabilizing at this value with higher increases in temperature of Sample SHT475. Correspondingly, only Fe-rich phase is observed in both samples, which is quite stable during solution treatment. Needless to say, the content of Fe-rich phase after sufficient solution treatment is 0.81 vol% and the decline of content of second phases due to dissolution of $Mg(Zn, Cu, Al)_2$ phase and soluble elements in Fe-rich phase is 2.38 vol%.

3.3 Effect of solution temperature on phase transformation

As mentioned before, the $S(Al_2CuMg)$ phase transforms from $Mg(Zn,Cu,Al)_2$ phase during solution treatment. In order to simplify the analysis, a hypothesis that diffusion coefficient is an exponential function which depends on the temperature is introduced. Hence, calculation equations of solid diffusion coefficient of Zn, Mg and Cu elements are deduced [14, 15] and detail information is shown in Table 5. The calculated results show that the diffusion coefficient of Zn element is almost five times bigger than that of Cu element. At low temperature, the Zn element of $Mg(Zn, Cu, Al)_2$ phase, approached to the interface between $Mg(Zn, Cu, Al)_2$ phase and the matrix, is dissolved into the matrix with a relatively higher diffusion rate compared with Cu element under the same surroundings. As solution treatment continues, reduction of Zn content

Table 5 Solid diffusion coefficient (D) of Cu, Mg and Zn elements during solution treatment ($m^2 \cdot s^{-1}$)

Elements	Calculated equation [7]	450 °C	460 °C	465 °C	470 °C	475 °C
Cu	$D = 4.8 \times 10^{-5}\exp(-16{,}069/T)$	1.074×10^{-14}	1.454×10^{-14}	1.952×10^{-14}	1.842×10^{-14}	2.256×10^{-14}
Mg	$D = 6.23 \times 10^{-6}\exp(-13{,}831/T)$	3.077×10^{-14}	3.994×10^{-14}	5.149×10^{-14}	4.896×10^{-14}	5.831×10^{-14}
Zn	$D = 2.45 \times 10^{-5}\exp(-14{,}385/T)$	5.625×10^{-14}	7.378×10^{-14}	9.608×10^{-14}	9.119×10^{-14}	1.093×10^{-13}
D_{Cu}:D_{Mg}:D_{Zn}		1.0:2.9:5.2	1.0:2.7:5.1	1.0:2.7:5.0	1.0:2.6:4.9	1.0:2.6:4.8

and accumulation of Cu content make the constituent of this area in accordance with S(Al_2CuMg) phase. As a result, S(Al_2CuMg) phase appears. Apparently, the nucleation and growth of S(Al_2CuMg) phase take place in the interface frontier of Mg(Zn, Cu, Al)$_2$ phase attached to the matrix, which is in accordance with the lamellar structure in Fig. 3d. In the present work, the S(Al_2CuMg) phase is found in SHT samples treated at 450, 460 and 465 °C.

However, with the solution temperature increasing, the diffusion rate gap between Zn and Cu is narrowed. That means that the diffusion coefficient of Zn element has no significant advantage to Cu element. So it becomes difficult to match the element proportion to form S(Al_2CuMg) phase. In other words, the Mg(Zn, Cu, Al)$_2$ phase is directly dissolved into the matrix during solution treatment. In present work, no S(Al_2CuMg) phase is found in SHT samples treated at 470 and 475 °C.

So it can be concluded that the formation of S(Al_2CuMg) phase is mainly controlled by the significant diffusion rate gap between Zn and Cu during solution treatment.

4 Conclusion

Solution temperature is the main factor influencing phase dissolution. The content of residual phases decreases with the increase of the solution temperature for the SHT samples. The S(Al_2CuMg) phase transforms from Mg(Zn, Cu, Al)$_2$ phase after solution-treated at 450, 460 and 465 °C, while the Mg(Zn, Cu, Al)$_2$ phase is directly dissolved into the matrix at 470 and 475 °C. The formation of S(Al_2CuMg) phase is mainly controlled by the significant diffusion rate gap between Zn and Cu during solution treatment.

Acknowledgments This study was financially supported by the National Program on Key Basic Research Project of China (No. 2012CB619504) and the National Natural Science Foundation of China (No. 51274046).

References

[1] Heinz A, Haszler A, Keidel C. Recent development in aluminium alloys for aerospace applications. Mater Sci Eng A. 2000;280(1):102.
[2] Srivatsan TS. Microstructure, tensile properties and fracture behaviour of aluminium alloy 7150. J Mater Sci. 1992;27(17):4772.
[3] Pierre A, David G. High temperature precipitation kinetics and TTT curve of a 7xxx alloy by in situ electrical resistivity measurements and differential calorimetry. Scr Mater. 2000;42(7):675.
[4] Dumont D, Deschamps A, Brechet Y. Characterisation of precipitation microstructures in aluminium alloys 7040 and 7050 and their relationship to mechanical behaviour. Mater Sci Eng A. 2004;20(5):567.
[5] Xu DK, Birbilis N, Lashansky D. Effect of solution treatment on the corrosion behaviour of aluminium alloy AA7150: optimisation for corrosion resistance. Corros Sci. 2011;53(1):217.
[6] Deng YL, Wan L, Zhang Y. Evolution of microstructures and textures of 7050 Al alloy hot-rolled plate during staged solution heat-treatments. J Alloys Compd. 2010;498(1):88.
[7] Han NM, Zhang XM, Liu SD. Effect of solution treatment on the strength and fracture toughness of aluminum alloy 7050. J Alloys Compd. 2011;509(10):4138.
[8] Robson JD. Microstructural evolution in aluminium alloy 7050 during processing. Mater Sci Eng A. 2004;382(1):112.
[9] Fang HC, Chen KH, Chen X. Effect of Cr, Yb and Zr additions on localized corrosion of Al–Zn–Mg–Cu alloy. Corros Sci. 2009;51(12):287.
[10] Morere B, Shahani R, Maurice C. The influence of Al_3Zr dispersoids on the recrystallization of hot-deformed AA 7010 alloys. Metall Mater Trans A. 2001;32(3):625.
[11] Mazibuko NE, Curle UA. Effect of solution heat treatment time on a rheocast Al–Zn–Mg–Cu alloy. Mater Sci Forum. 2011;690:343.
[12] Underwood EE. Quantitative Stereology. Reading: Addison-Wesley; 1970. 68.
[13] Wang H, Xu J, Kang Y. Study on inhomogeneous characteristics and optimize homogenization treatment parameter for large size DC ingots of Al–Zn–Mg–Cu alloys. J Alloys Compd. 2014;585:19.
[14] Xie F, Yan X, Ding L. A study of microstructure and microsegregation of aluminum 7050 alloy. Mater Sci Eng A. 2003;355(1):144.
[15] Wei B, Herlach DM, Feuerbacher B. Dendritic and eutectic solidification of undercooled Co Sb alloys. Acta Metall Mater. 1993;41(6):1801.